Numerical and SVM-based Analysis of CO and CO_2 Production in the Slag Fuming Furnace: Influence of Operational Conditions

Mehrdad Mesgarpour[1], Sasan Sadrizadeh[1,2], Konstantinos G. Kyprianidis[1], Rebei Bel Fdhila[1,4]

[1]School of Business, Society and Engineering, Mälardalens University, Universitetsplan 1, 722 20, Västerås, Sweden, mehrdad.mesgarpour@mdu.se , konstantinos.kyprianidis@mdu.se
[2] Department of Civil and Architectural Engineering, KTH Royal Institute of Technology, Stockholm, Sweden, ssad@kth.se
[3]Hitachi Energy Research, Forskargränd 7, 72178 Västerås, Sweden, rebei.bel.fdhila@mdu.se

Keywords: Fuming Process, CO/CO2 Production, Slag, Support Vector Machine

Abstract. The slag fuming process is a metallurgical technique for zinc recovery, driven by reduction reactions through air and coal injection. This study investigates the formation rates of CO and CO_2 under various operational conditions by integrating high-resolution numerical simulations with Support Vector Machine (SVM) modeling for predictive analysis. In present study, air and coal are injected at 100 *m/s* and 500 K into slag maintained at 1,500 *K*, which consists of varying volume fractions of ZnO, Al_2O_3, Fe_2O_3, SiO_2, and FeO. The coal injection rate is fixed at 0.09 *kg/s*, whereas air mass flow rates are varied to evaluate their influence on gas generation. A Eulerian multiphase model simulates the interactions between slag, air, and coal within a 5.0 *m* × 2.4 *m* × 0.6 *m* furnace. Additionally, the S-Gamma population balance model resolves bubble dynamics, including gas generation and coalescence phenomena. SVM modeling provides a predictive framework for CO and CO_2 evolution, accounting for nonlinear dependencies on air and coal mass flow rates. Through the combination of numerical simulation and machine learning, this research offers insights into optimizing slag-fuming processes. The results indicated that, as the nozzle Reynolds number increases from approximately 114,812.61 to 157,867.34, the final CO_2 production ratio grows from 4.079 to 4.649.

1. Introduction

Copper slag, a byproduct generated during the smelting of copper, presents both a challenge and an opportunity. While it represents a significant waste stream, it also contains valuable metals and has the potential to be utilized as a resource. Copper slag typically contains a complex mixture of oxides, including significant amounts of iron oxide (FeO), silica (SiO_2), and alumina (Al_2O_3), along with lesser amounts of zinc oxide (ZnO), lead oxide (PbO), and other metal oxides. The exact composition varies depending on the mining location and smelting process. These oxides influence the physical properties of the slag, such as its viscosity and melting point, which in turn affect the efficiency of the fuming process [1]. Combustion of coal generates heat and carbon monoxide (CO), creating a reducing environment within the furnace. This process involves several key reactions. Firstly, the coal combusts and undergoes gasification. The generated carbon monoxide then participates in the reduction of metal oxides within the slag. ZnO is reduced to metallic Zn by the reaction: Similarly, PbO is reduced by the reaction: FeO are also reduced. Furthermore, metallic iron, produced from the reduction of Fe_3O_4, can also contribute to the reduction of ZnO. The metallic Zn and Pb produced in these reactions vaporize due to the high temperatures in the furnace [2, 3].

The application of Support Vector Machines (SVMs) to predict CO and CO_2 emissions within fuming furnaces necessitates a comprehensive review of relevant literature spanning several key domains. Primarily, the inherent non-linearities of fuming furnace processes demand robust predictive models, making SVMs, particularly through Support Vector Regression (SVR), a promising approach.

Foundational literature on general SVM applications in industrial process modeling provides crucial insights. Research detailing SVR's efficacy in complex industrial systems establishes its suitability for handling the intricate relationships characteristic of metallurgical processes [4]. Studies focusing on SVM-driven process optimization and control further demonstrate its potential to enhance efficiency and reduce process variability, critical considerations for emission mitigation. The field of machine learning for emissions prediction offers direct relevance [5].

In the present study, the slag fuming process involving coal-based reduction is investigated to identify patterns of CO and CO_2 production over a 1-hour simulation period. Due to the numerous chemical reactions occurring within the slag bath and air zone, a complex Multiphysics model is developed using the Eulerian approach, reaction models, and a series of user-defined functions (UDFs) to accurately simulate the process. Following the numerical modeling, the simulation results are employed in a SVM analysis to illustrate the influence of operational conditions on the time-dependent CO and CO_2 production rates.

2. Problem statement and methodology

To examine the effects of the nozzle velocities on CO/CO_2 production rate, a 3D Slag-fuming Furnace (SFF) model is employed, as illustrated in Figures 1a and 1b. This figure depicts two submerged nozzles ($D_n = 50$ *mm*) positioned on the sidewalls, 100 *mm* above the bottom. A mixture of high-pressure air (O_2 and N_2) and coal particles is introduced through the tuyere. The SFF has a height of 5,000 *mm*, with walls 300 *mm* thick to minimize computational demands. Symmetry conditions are applied to both sides of the SFF, while all other surfaces are treated as walls. In this study, the slag comprises different components, each with specific volume fractions. In present study, the composition of slag is based on HUDA et al.{Huda, 2012 #1204} . The slag level is maintained at 1,000 *mm*, and the components, along with the average properties of the slag, are detailed in Ref.[6] . The modelling of air jets incorporating coal particles into slag necessitates the Eulerian approach for multi-phase flow analysis. Additionally, a population model is used to determine the distribution of bubbles during the process. This methodology was applied to model interactions between solid-gas and gas-liquid phases. In the main simulation, the air is channeled through two tuyeres at a V_{nozzle}=100 *m/s* each, $\boldsymbol{\rho}$ =990 kg/m^3. The coal particles are assumed to be spherical with an average diameter of 100 μm. Throughout the process, the temperatures of both slag and air are kept constant (T_{slag}= 1,220 *K*, T_{air} = 500 *K*). To prevent melting, a cooling jacket providing a constant heat flux of 5 *MW* is placed around the furnace. In the present study, the viscosity of air and slag are $\boldsymbol{\mu}$ = 1.7894e-05, 0.152 *Pa.s*, while the density of air, coal, and slag in the main model are 1225, 990, and 3,400 kg/m^3, respectively.

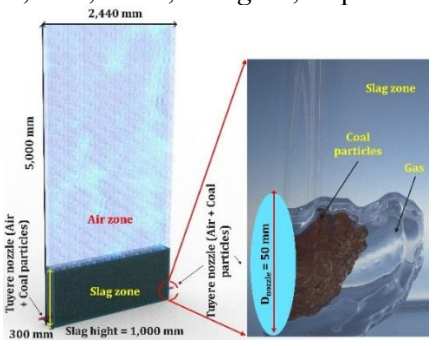

(a)

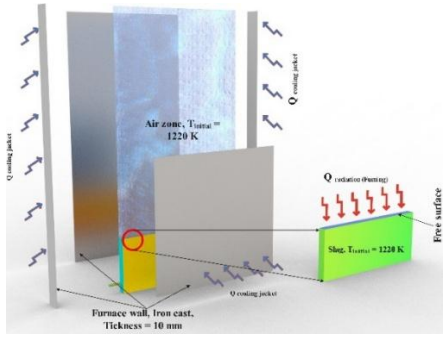

(b)

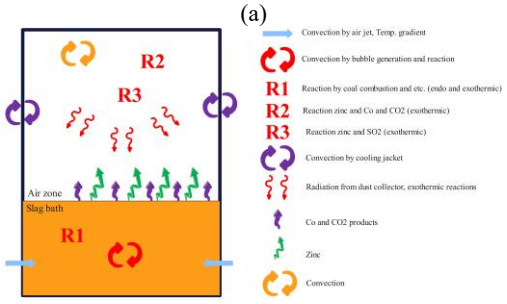

(c)

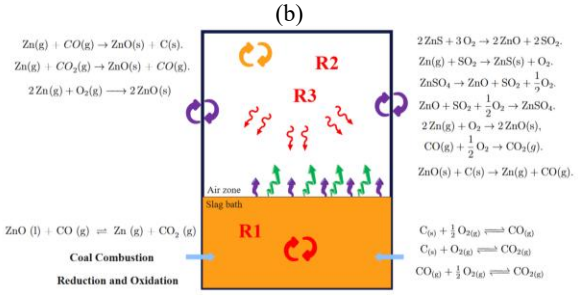

(d)

Figure 1 Graphical illustration of a) SFF geometry and dimensions, b) boundary conditions, c) schematics of heat and mass transfer and d) Endo and Exothermic reactions

For the surface tension between air and slag, surface tension is considered a constant value of 0.43 *N/m*. A graphical schematic of the heat transfer network, illustrating an iron cast wall with a 10 mm thickness cooled from all sides by a liquid-based jacket, is provided in Figure 1b. The heat from the top of the furnace raises the slag's top surface temperature, with radiation modelled as a constant heat flux of 5 *kW*. A graphical representation of heat transfer and the reaction model in the air zone and slag bath is shown in Figures 1c and 1d.

3. Governing Equations

The conservation of mass in Eulerian model [7]:

$$\frac{\partial}{\partial t}\left(\alpha_q \rho_q\right) + \nabla \cdot \left(\alpha_q \rho_q \overrightarrow{v_q}\right) = \sum_{p=1}^{n}\left(\dot{m_{pq}} - \dot{m_{qp}}\right) + S_q \tag{1}$$

where α_q is cell value of volume fraction, ρ_q is density of phase q, $\overrightarrow{v_q}$ is mass-averaged velocity of phase q, $\dot{m_{pq}}$ is mass transfer from phase q to phase p, S_q is source of enthalpy. For the conservation of momentum [8]:

$$\frac{\partial}{\partial t}\left(\alpha_q \rho_q \overrightarrow{v_q}\right) + \nabla \cdot \left(\alpha_q \rho_q v_q \overrightarrow{v_q}\right) = -\alpha_q \nabla p + \nabla \cdot \overrightarrow{\tau_q} + \alpha_q \rho_q \vec{g} + \sum_{p=1}^{n}\left(\overrightarrow{R_{pq}} + \dot{m_{pq}}\overrightarrow{v_{pq}} - \dot{m_{qp}}\overrightarrow{v_{qp}}\right) + \left(\overrightarrow{F_q} + \overrightarrow{F_{lift,q}} + \overrightarrow{F_{wl,q}} + \overrightarrow{F_{vm,q}} + \overrightarrow{F_{td,q}}\right) \tag{2}$$

where p is pressure, $\overrightarrow{R_{pq}}$ is interaction force between phases, $\overrightarrow{v_{pq}}$ is interphase velocity, $\overrightarrow{F_q}$ is external force, $\overrightarrow{F_{lift,q}}$ is lift force of phase q, $\overrightarrow{F_{wl,q}}$ is wall lubrication force, $\overrightarrow{F_{vm,q}}$ is virtual mass force of Eulerian phase, $\overrightarrow{F_{td,q}}$ is turbulence dispersion force. Also $\overrightarrow{\tau_q}$ is defined as:

$$\overrightarrow{\tau_q} = \alpha_q \mu_q \left(\nabla \overrightarrow{v_q} + \left(\nabla \overrightarrow{v_q}\right)^T\right) + \alpha_q \lambda_q \left(\frac{2}{3}\mu_q\right)\left(\nabla \cdot \overrightarrow{v_q}\right)\vec{I} \tag{3}$$

where μ_q represents viscosity of phase q, λ_q denotes viscosity of phase q. The conservation of energy is:

$$\frac{\partial}{\partial t}\left(\alpha_q \rho_q h_q\right) + \nabla \cdot \left(\alpha_q \rho_q \overrightarrow{u_q} h_q\right) = \alpha_q \frac{dp_q}{dt} + \overrightarrow{\tau_q} : \nabla \overrightarrow{u_q} - \nabla \cdot \overrightarrow{q_q} + S_q + \sum_{p=1}^{n}\left(Q_{pq} + \dot{m_{pq}} h_{pq} - \dot{m_{qp}} h_{qp}\right) - \nabla \cdot \sum_j h_{j,q}\overrightarrow{J_q} \tag{4}$$

where h_q is Specific enthalpy of the q^{th} phase, $\overrightarrow{u_q}$ is velocity of phase q, Q_{pq} is interphase enthalpy, h_{pq} is specific enthalpy of phase p to phase q, $h_{j,q}$ is enthalpy of species and $\overrightarrow{J_q}$ is diffusive flux of species. For the fluid-solid momentum equations:

$$\frac{\partial}{\partial t}\left(\alpha_s \rho_s \overrightarrow{v_s}\right) + \nabla \cdot \left(\alpha_s \rho_s \overrightarrow{v_s}\overrightarrow{v_s}\right) = -\alpha_s \nabla p - \nabla p_s + \overrightarrow{\tau_s} : \nabla \overrightarrow{v_s} + \alpha_s \rho_s \vec{g} + \sum_{l=1}^{N}\left(K_{ls}\left(\overrightarrow{v_l} - \overrightarrow{v_s}\right) + \dot{m_{ls}}\overrightarrow{v_{ls}} - \dot{m_{sl}}\overrightarrow{v_{sl}}\right) + \left(\overrightarrow{F_s} + \overrightarrow{F_{lift,s}} + \overrightarrow{F_{vm,s}} + \overrightarrow{F_{td,s}}\right) \tag{5}$$

where K_{ls} is momentum exchange coefficient between fluid or solid phase. Reynolds-Averaged Navier-Stokes (RANS) turbulence models provide closure relations for the RANS equations that govern the transport of the mean flow quantities. The constant rate devolatilization law dictates that volatiles are released at a constant rate:

$$-\frac{1}{f_{v,0}\left(1 - f_{w,0}\right)m_{p,0}}\frac{dm_p}{dt} = A_0 \tag{6}$$

where dm_p is particle mass, $f_{w,0}$ is the fraction of volatiles initially present in the particle. $m_{p,0}$ is initial particle mass, and A_0 is rate constant.

After establishing the governing equations for multiphase interactions, SVM is employed to model and predict CO and CO_2 production. The SVM is a supervised learning algorithm used for classification and regression tasks. To extend SVM to nonlinear problems, the optimization problem is rewritten using lagrange multipliers α_i, allowing the use of kernel functions [9]:

$$max_{\alpha} \sum_{i=1}^{N} \alpha_i - \frac{1}{2} \sum_{i=1}^{N} \sum_{j=1}^{N} \alpha_i \alpha_j y_i y_j K(x_i, x_j) \quad (7)$$

4. Grid study and Validation

In the present study, a mosaic mesh was generated in the computational domain to enhance accuracy. Figure 2a presents the variation of dimensionless temperature and velocity concerning the number of cells. The results indicate an optimal cell count, minimizing velocity variation around 6.8E6, while the corresponding value for temperature is approximately 9E6.
Another important parameter in transient modelling is the Courant number (CFL) study, which is represented in Figure 2b. The Courant number and residual of volume fraction were considered as key parameters for this study. The results show that a time step of 5E-06 seconds is suitable for this case.

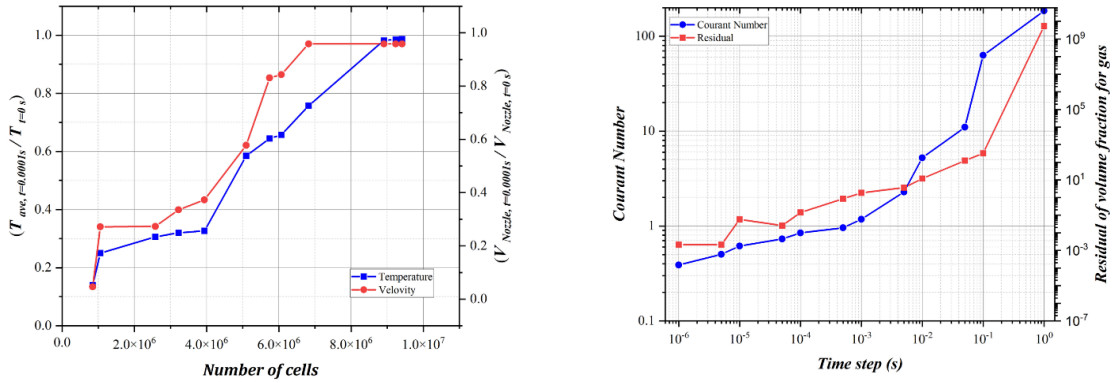

(a) (b)

Figure 2 a) Grid study, and b) CFL analysis

In the present study, the modelling results were compared with the outcomes of HUDA et al. [10]. According to Figure 3, for this comparison, two criteria (slag velocity and coal mass) were used in a data harvesting line from the middle of the nozzle to the middle of the furnace. The results indicated that the maximum error for slag velocity is below 14%, and for the mass of coal, it is 16.44 %.

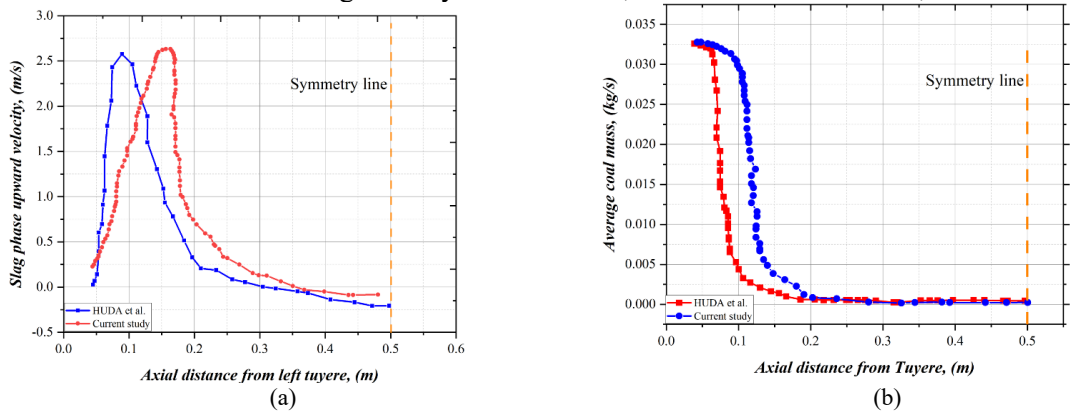

(a) (b)

Figure 3 Comparison current study results for a) slag phase upward velocity, and b) average coal mass with HUDA et al. [10]

5. Results and Discussion

Kinetically, the oxidation of Zn vapor in CO/CO_2 mixtures is a heterogeneous process that occurs on interfaces, and the reaction rates are governed by chemical mechanisms rather than mass transport. The composition of the gas mixture plays a crucial role in determining the dominant oxidation pathway. Higher CO/CO_2 ratios Favor oxidation by CO, leading to finer ZnO morphology, whereas lower ratios promote CO_2 driven oxidation, resulting in coarser deposits. Morphological variations are evident, with

coarse ZnO deposits forming at low temperatures (below 800°C), fine ZnO deposits at high temperatures (above 900°C), and intermediate morphologies appearing around 900 °C at moderate CO/CO_2 ratios. Additionally, the reaction rate is found to be zero-order with respect to the concentrations of Zn, CO, and CO_2, indicating that the reaction sites on the surface are saturated. From a thermodynamic perspective, both oxidation reactions are viable under the experimental conditions. Free energy ΔG calculations show that the reaction with CO_2 is typically dominant at the air zone of SFF, where CO_2 partial pressure is higher. As the gas mixture progresses through the SFF, CO partial pressure increases, making CO-driven oxidation more significant. Temperature critically influences oxidation pathways. CO_2 oxidation favoured at lower temperatures and CO oxidation more accessible at higher temperatures, even when it is less thermodynamically favoured.

The Boudouard reaction plays a vital role specifically in the air zone (oxidation zone) of an SFF, directly influencing overall furnace performance and Zn recovery efficiency. In the air zone, injected air combusts carbonaceous reductants (such as coal or coke), initially producing CO_2. Subsequently, at temperatures typically between 800 and 1200 °C, the Boudouard reaction ($C + CO_2 \leftrightarrow 2CO$) occurs, converting CO_2 back into CO, a highly effective reducing gas. This in-situ regeneration of CO is particularly crucial, as it ensures a continuous supply of reducing atmosphere deeper into the slag bath, effectively reducing ZnO to metallic Zn vapor. Without the Boudouard reaction, the reducing potential of the gas atmosphere would diminish rapidly due to CO oxidation, limiting ZnO reduction and thus lowering the overall recovery of Zn. Figures 4a and 4b show the dimensionless production of CO and CO2 at the end of the simulation. The results indicated that, concentration of CO/CO_2 has more concentration close to interface of slag bath and the air side.

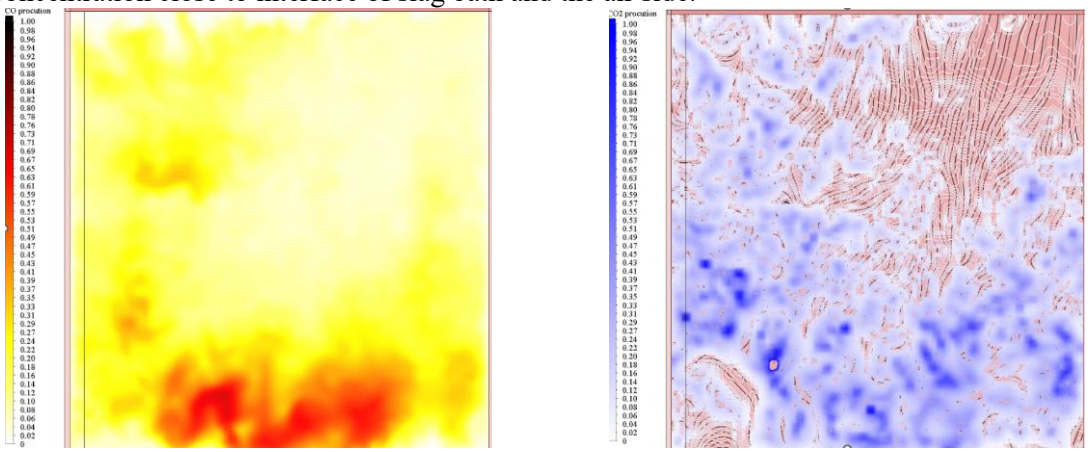

(a) (b)

Figure 4 Dimensionless contours $\left(\frac{Average\ of\ CO/CO_2\ mass\ (kg)}{Total\ production\ of\ CO/CO_2\ over\ 1\ hr(kg)}\right)$ of a) CO and b) CO_2 production overt time

Table 1 presents dimensionless results for CO and CO_2 formation and reduction at four different nozzle Reynolds numbers, each value normalized by the coal mass flow over one hour. As the nozzle Reynolds number increases from approximately 114,812 to 157,867, the overall trend indicates that both CO_2 and CO production rise. Specifically, the final CO_2 ratio grows from 4.079 to 4.649, while the final CO ratio increases from 9.348 to 9.808. The "CO_2 Reduced" term, which reflects how much CO_2 is consumed by reduction reactions before exiting the system, remains fairly steady around 1.73 to 1.75, suggesting that the net consumption of CO_2 by reductive pathways does not vary substantially with increasing turbulence. However, the steady rise in final CO_2 points to enhanced oxidation overall, likely driven by better mixing and higher local reaction rates at elevated Reynolds numbers. A closer look at specific reaction pathways underscores how improved flow conditions affect chemical transformations. CO produced by the Boudouard reaction increases from 2.51 to 3.70, while CO generated through general reduction also rises from 5.84 to 6.64. Taken together, these changes highlight the dual influence of enhanced mixing, which both accelerates oxidation (evidenced by higher final CO_2) and promotes various reduction reactions (seen in the increased CO yields).

Table 1 SVM results for variation of Re at the nozzle

Re_{Nozzle}	$\left(\frac{CO_{2,Reduced}}{\dot{m}_{coal,1hr}}\right)$	$\left(\frac{CO_{2,Final}}{\dot{m}_{coal,1hr}}\right)$	$\left(\frac{CO_{Final}}{\dot{m}_{coal,1hr}}\right)$	$\left(\frac{CO_{Boudouard}}{\dot{m}_{coal,1hr}}\right)$	$\left(\frac{CO_{Reduction}}{\dot{m}_{coal,1hr}}\right)$	$\left(\frac{CO_{2,Reduction\ of\ ZnO}}{\dot{m}_{coal,1hr}}\right)$
114,812.61	1.752	4.090	9.348	3.505	5.843	2.919
129,164.18	1.745	4.273	9.509	3.490	6.018	3.001
143,515.76	1.734	4.459	9.662	3.468	6.193	3.094
157,867.34	1.719	4.649	9.808	3.439	6.368	3.182

6. Conclusion

In the present study, we integrate a Support Vector Machine (SVM) framework with high-resolution numerical simulations to assess the impact of varying operational conditions, such as airflow rate and injection parameters, on CO and CO_2 formation in slag fuming. The 3D Eulerian multiphase model captures the underlying reaction and bubble dynamics effectively, while SVM predictions provide insights into emission trends under different working conditions. This integrated approach offers a robust method for optimizing Zn recovery processes. The results indicate that:

1- The oxidation of Zn vapor in CO/CO_2 mixtures is governed by chemical kinetics on interfaces, not mass transport. Tthe CO/CO_2 ratio strongly influences ZnO morphology (finer deposits at higher CO/CO_2 ratios and coarser ones at lower ratios).
2- In the air zone of the SFF, the Boudouard reaction ($C + CO_2 \leftrightarrow 2CO$) is pivotal for regenerating CO, maintaining a robust reducing atmosphere that sustains ZnO reduction to metallic Zn vapor. Without this reaction, the reducing potential would drop rapidly, limiting Zn recovery.
3- Dimensionless analyses at different nozzle Reynolds numbers show that enhanced turbulence increases both CO_2 (via oxidation) and CO (via reduction), underscoring the dual effect of mixing. Here, the SVM model provides predictive insight into how variations in operational parameters such as flow rates and injection conditions affect CO/CO_2 formation, offering a valuable tool for optimizing slag fuming processes.

6. References

1. Nagraj, S., M. Chintinne, M. Guo, and B. Blanpain. *Slag Fuming Process-A Review*. in *International Process Metallurgy Symposium (IPMS 2019)*. 2019.
2. Richards, G.G., J. Brimacombe, and G. Toop, *Kinetics of the zinc slag-Fuming process: Part i. industrial measurements.* Metallurgical Transactions B, 1985. **16**: p. 513-527.
3. Wiafe, J.E., *Equilibria and kinetics of zinc fuming from slags.* 1984.
4. Li, Q., C. Liu, and Q. Guo, *Support vector machine with robust low-rank learning for multi-label classification problems in the steelmaking process.* Mathematics, 2022. **10**(15): p. 2659.
5. Gürsoy-Demir, H. and M. Ozturk, *Deep learning and supervised learning techniques for modeling and prediction of strength of ground granulated blast furnace slag based sustainable mortar.* Neural Computing and Applications, 2025. **37**(3): p. 1709-1726.
6. Huda, N., J. Naser, G. Brooks, M.A. Reuter, and R. Matusewicz, *Computational fluid dynamics (CFD) investigation of submerged combustion behavior in a tuyere blown slag-fuming furnace.* Metallurgical and Materials Transactions B, 2012. **43**(5): p. 1054-1068.
7. Passman, S.L., J.W. Nunziato, and E.K. Walsh, *A theory of multiphase mixtures*, in *Rational thermodynamics*. 1984, Springer. p. 286-325.
8. Subramaniam, S., *Lagrangian–Eulerian methods for multiphase flows.* Progress in Energy and Combustion Science, 2013. **39**(2-3): p. 215-245.
9. Somvanshi, M., P. Chavan, S. Tambade, and S. Shinde. *A review of machine learning techniques using decision tree and support vector machine*. in *2016 international conference on computing communication control and automation (ICCUBEA)*. 2016. IEEE.
10. Huda, N., J. Naser, G. Brooks, M.A. Reuter, and R.W. Matusewicz, *Computational fluid dynamic modeling of zinc slag fuming process in top-submerged lance smelting furnace.* Metallurgical and Materials Transactions B, 2012. **43**: p. 39-55.